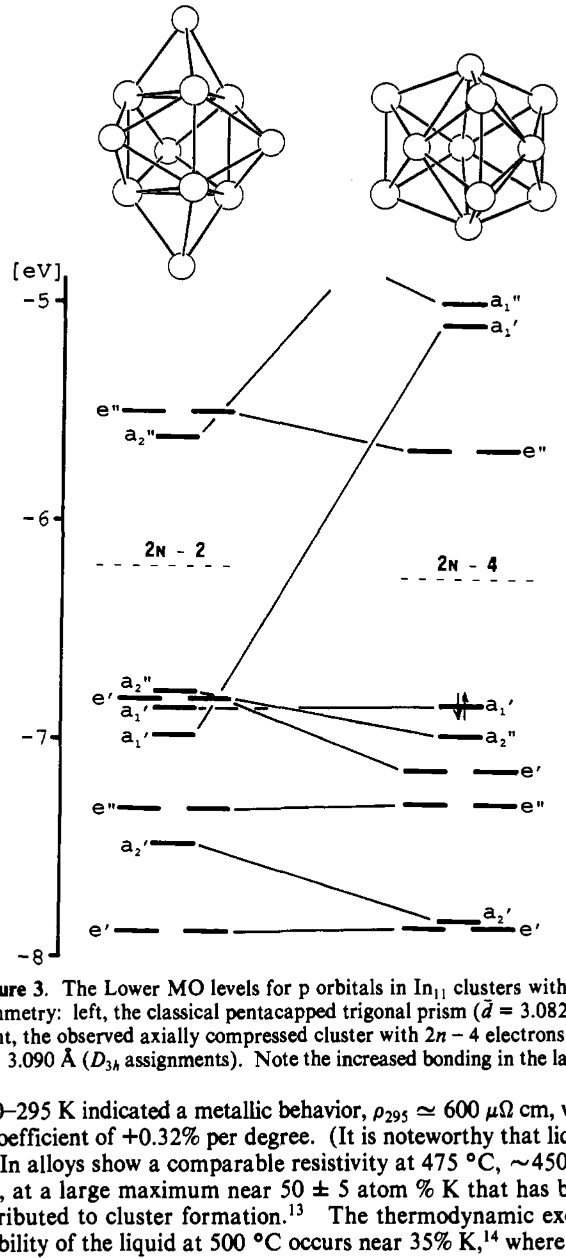

Figure 3. The Lower MO levels for p orbitals in In_{11} clusters with D_{3h} symmetry: left, the classical pentacapped trigonal prism ($\bar{d}$ = 3.082 Å); right, the observed axially compressed cluster with $2n - 4$ electrons and $\bar{d}$ = 3.090 Å (D_{3h} assignments). Note the increased bonding in the latter.

110–295 K indicated a metallic behavior, $\rho_{295} \simeq 600$ μΩ cm, with a coefficient of +0.32% per degree. (It is noteworthy that liquid K–In alloys show a comparable resistivity at 475 °C, ~450 μΩ cm, at a large maximum near 50 ± 5 atom % K that has been attributed to cluster formation.[13] The thermodynamic excess stability of the liquid at 500 °C occurs near 35% K,[14] where the solid system has a network structure $K_{22}In_{39}$).

We conclude that one electron per cluster is delocalized, probably over the double K1 layers (perhaps with antibonding In–In contributions) in which the shortest interlayer K–K distances, 4.05 Å, are comparable to the single-bond value, 4.00 Å.[6] The need for an extra potassium atom must arise from packing requirements and "solvation" of the polyanion by sufficient cations; intercalation of these layers by one halide per K_8In_{11} has not been successful. Substitution reactions with sodium have given other phases. On the other hand, the larger cation in RbK_7In_{11} disorders in half of the K2 positions with expansion of only the *a–b* (cluster) net, while two more rubidium atoms appear to complete the K2 substitution and randomly occupied one-sixth of the K1 sites with a substantial lattice expansion in *c*.

The In_{11}^{7-} ion represents a new cluster-bonding configuration in an evidently unknown hypoelectronic (homoatomic) cluster regime. An analogue of the better known C_{2v} closo deltahedron with 11 vertices and 24 electrons (as for $B_{11}H_{11}^{2-}$) would require an unreasonable -13 charge with In_{11}. This charge problem is alleviated for many gallium (and indium) clusters through the formation of network structures via intercluster bonds, e.g., at all 11 vertices of the ideal C_{2v} Ga_{11} unit in K_3Ga_{13}.[15] The only alternative mentioned in the literature appears to be ideal pentacapped trigonal prism, but this is thought to be disfavored by the presence of two vertices of order 3.[16] According to extended Hückel calculations,[17] the latter cluster exhibits a 1.2-eV HOMO–LUMO gap with only 20 p electrons ($2n - 2$).[18] The axial compression and lateral expansion necessary to achieve the observed ($2n - 4$) cluster (Figure 3) drives a single bonding a_1' orbital higher via both loss of bonding in the ends of the trigonal prism and increased antibonding In1–In2 interactions, while several occupied levels become more stable.

The general assessment of alkali-metal–indium compounds (AB_x) as similar to gallium examples appears to be unwarranted. There are some isostructural AB_4 and AB (NaTl-type) examples and common network structures for the pairs $CsGa_3$–$CsIn_3$[19–21] and $Na_{21}Ga_{39}^{3}$–$K_{22}In_{39}$.[23] The many evidently unique indium examples are presently under study. We also find that the unreported phase Na_2In exists and is isostructural with Na_2Tl.[24] This makes it formally a Zintl phase and another cluster example, as it contains isolated In_4 tetrahedra with edges of 3.066 (2)–3.153 (1) Å that are isoelectronic with Sn_4^{4-} in KSn,[25] Sb_4(g), P_4, etc. Isolated gallium polyhedra are not known in any alkali-metal compound, although Ga_3 and Ga_4 units occur in Ba_8Ga_7.[26]

Supplementary Material Available: Tables giving data collection and refinement information, atom parameters, and distances and angles for K_8In_{11} (4 pages); a listing of observed and calculated structure factor results for the same compound (5 pages). Ordering information is given on any current masthead page.

Ames Laboratory—DOE[27] and
Department of Chemistry
Iowa State University
Ames, Iowa 50011

Slavi C. Sevov
John D. Corbett*

Received July 24, 1991

---

(13) Meijer, J. A.; Geertsma, W.; van der Lugt, W. *J. Phys. F.: Met. Phys.* **1985**, *15*, 899.
(14) Takenaka, T.; Petric, A.; Saboungi, M.-L. *J. Phys.: Condens. Matter* **1991**, *3*, 1603.
(15) Belin, C.; Ling, R. G. *J. Solid-State Chem.* **1983**, *48*, 40.
(16) King, R. B.; Rouvray, D. H. *J. Am. Chem. Soc.* **1977**, *99*, 7834.
(17) Orbital parameters and energies from: Janiak, C.; Hoffmann, R. *J. Am. Chem. Soc.* **1990**, *112*, 5924. Predominantly s-based orbitals in a cluster with the observed dimensions lie between −17.7 and −9.0 eV, while the higher block of nine bonding orbitals have on average only 2.5% In 5s population.
(18) We were reminded that this closed-shell count can be easily derived by the addition of two axial In^+ ions to the closo In_9^{11-} (D_{3h}) ion, which adds no new bonding orbitals or p electrons (Burdett, J. K. Private communication).
(19) Ling, R. C.; Belin, C. *Z. Anorg. Allg. Chem.* **1981**, *480*, 181.
(20) Van Vucht, J. H. N. *J. Less-Common Met.* **1985**, *108*, 163.
(21) Tschuntonow, K. A.; Yatsenko, S. P.; Hryn, Yu. N.; Yarmolyuk, Ya. P.; Orlov, A. N. *J. Less-Common Met.* **1984**, *99*, 15.
(22) Reference deleted in proof.
(23) Sevov, S. C.; Corbett, J. D. Unpublished results.
(24) Hansen, D. A.; Smith, J. F. *Acta Crystallogr.* **1967**, *22*, 836.
(25) Hewaidy, I. F.; Busmann, E.; Klemm, W. *Z. Anorg. Allg. Chem.* **1964**, *328*, 283.
(26) Fornasini, M. L. *Acta Crystallogr.* **1983**, *C39*, 943.
(27) Ames Laboratory—DOE is operated for the U.S. Department of Energy by Iowa State University under Contract No. W-7405-Eng-82. This research was supported by the Office of Basic Energy Sciences, Materials Sciences Division.

A Model for the Substrate Adduct of Copper Nitrite Reductase and Its Conversion to a Novel Tetrahedral Copper(II) Triflate Complex

Denitrification, the dissimilatory transformation of NO_3^- and NO_2^- to gaseous nitrous oxide (N_2O) and/or dinitrogen, is a central process in the biological nitrogen cycle responsible for depletion from soil of nitrogen necessary for plant growth and

0020-1669/91/1330-4877$02.50/0 © 1991 American Chemical Society

Scheme I

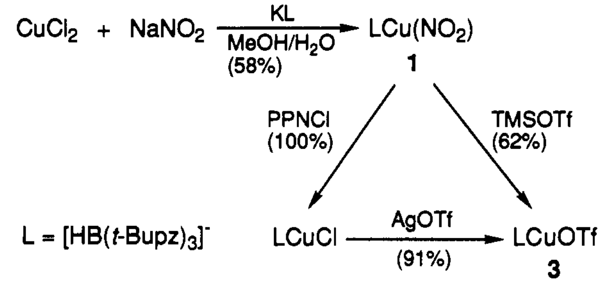

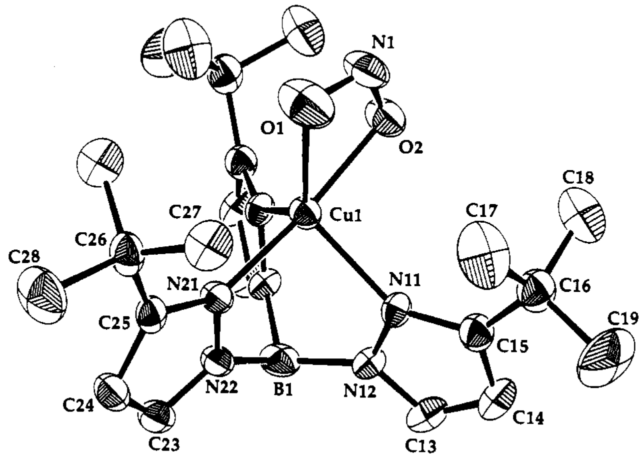

Figure 1. ORTEP drawing of **1** showing the 40% probability thermal ellipsoids and atom labels for all non-hydrogen atoms. Selected interatomic distances (Å) and angles (deg) are as follows: Cu1–N11, 2.100 (4); Cu1–N21, 1.954 (5); Cu1–O1, 2.169 (6); Cu1–O2, 1.976 (5); N1–O1, 1.239 (8); N1–O2, 1.246 (8); N11–Cu1–N11′, 102.0 (2); N11–Cu1–N21, 90.1 (2); N11–Cu1–O1, 126.0 (1); N11–Cu1–O2, 96.5 (1); N21–Cu1–O1, 110.8 (2); N21–Cu1–O2, 169.5 (2); O1–Cu1–O2, 58.7 (2); O1–N1–O2, 110.1 (6).

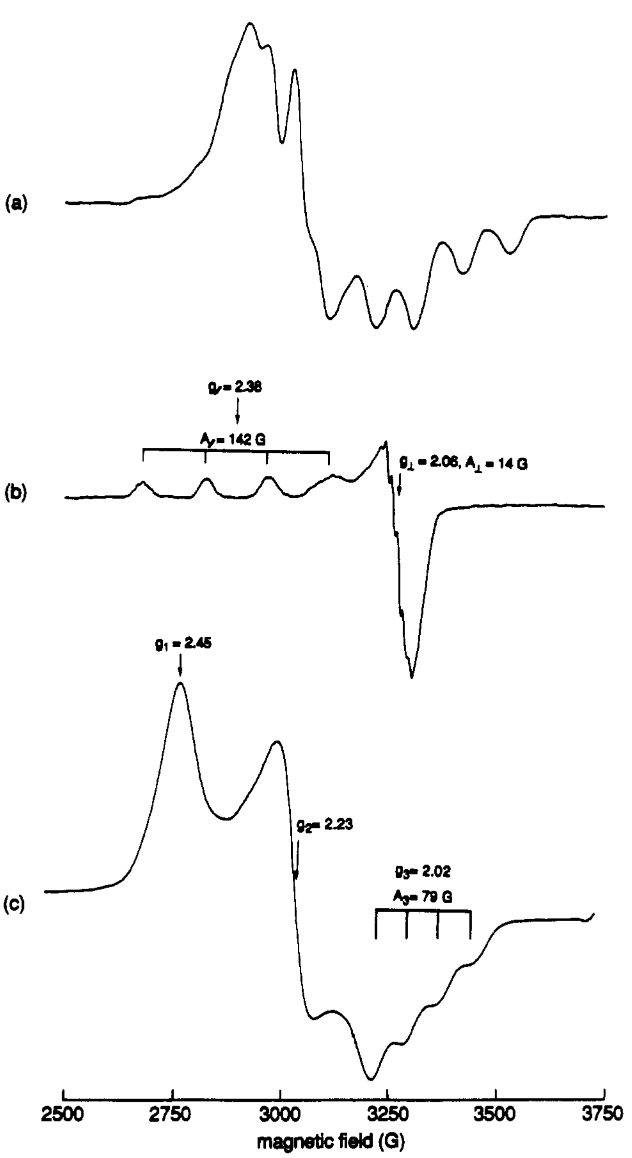

Figure 2. X-Band EPR spectra of (a) **1**, (b) **2**, and (c) **3** (all as CH_2Cl_2–toluene glasses, 77 K).

production of a substance, N_2O, believed to contribute to global warming and atmospheric ozone loss.[1] Conversion of NO_2^- to NO and/or N_2O is performed by the nitrite reductases (NiR), one of which (the enzyme from *Achromobacter cycloclastes*)[2–4] has recently been shown by a 2.3-Å resolution X-ray crystal structure to contain two well-separated copper ions (Cu⋯Cu = 12.5 Å), one metal being bound to ligands typical for type 1 centers, the other presumably catalytic copper ion being coordinated by three histidines and a small, probably aquo, moiety in an unusual tetrahedral array.[3] Mechanistic experiments on this enzyme using isotopically labeled substrates and trapping reagents were interpreted to indicate that nitrite reduction occurs via a sequence initially involving binding to copper, probably at the pseudotetrahedral site,[3] followed by dehydration to form a copper nitrosyl intermediate (eq 1).[1,4]

$$\text{E–Cu} \xrightarrow{\text{NO}_2^-} \text{E–Cu–NO}_2^- \xrightarrow{+2\text{H}^+,\ -\text{H}_2\text{O}} \text{E–Cu–NO}^+ \qquad (1)$$

While ample precedent in the form of model chemistry for the species in eq 1 exists for other metals,[5] most notably for iron in a heme environment,[5d–k] synthetic analogs that adequately support the viability of the proposed monocopper adducts have not been prepared.[6–8] Here I report the synthesis and structural charac-

---

(1) (a) *Denitrification, Nitrification, and Atmospheric Nitrous Oxide*; Delwiche, C. C., Ed.; John Wiley & Sons: New York, 1981. (b) *Denitrification in the Nitrogen Cycle*; Golterman, H. L., Ed.; Plenum Press: New York, 1983. (c) Payne, W. J. *Denitrification*; John Wiley & Sons: New York, 1981. (d) Hochstein, L. I.; Tomlinson, G. A. *Annu. Rev. Microbiol.* **1988**, *42*, 231–261.

(2) (a) Dooley, D. M.; Moog, R. S.; Liu, M.-Y.; Payne, W. J.; LeGall, J. *J. Biol. Chem.* **1988**, *263*, 14625–14628. (b) Iwasaki, H.; Noji, S.; Shidara, S. *J. Biochem.* **1975**, *78*, 355–361. (c) Turley, S.; Adman, E. T.; Sieker, L. C.; Liu, M.-Y.; Payne, W. J.; LeGall, J. *J. Mol. Biol.* **1988**, *200*, 417–419. (d) Iwasaki, H.; Matsubara, T. *J. Biochem.* **1972**, *71*, 645–652. (e) Liu, M.-Y.; Liu, M.-C.; Payne, W. J.; LeGall, J. *J. Bacteriol.* **1986**, *166*, 604–608.

(3) Godden, J. W.; Turley, S.; Teller, D. C.; Adman, E. T.; Liu, M.-Y.; Payne, W. J.; LeGall, J. *Science* **1991**, *253*, 438–442.

(4) (a) Hulse, C. L.; Averill, B. A.; Tiedje, J. M. *J. Am. Chem. Soc.* **1989**, *111*, 2322–2323. (b) Ye, R. W.; Toro-Suarez, I.; Tiedje, J. M.; Averill, B. A. *J. Biol. Chem.* **1991**, *266*, 12848–12851. (c) Jackson, M. A.; Tiedje, J. M.; Averill, B. A. *FEBS Lett.* **1991**, *291*, 41. Controversy surrounds the steps subsequent to those shown in eq 1, however; see, for example: Goretski, J.; Hollocher, T. C. *J. Biol. Chem.* **1990**, *265*, 889–895 and references therein.

(5) (a) Godwin, J. B.; Meyer, T. J. *Inorg. Chem.* **1971**, *10*, 2150–2153. (b) Rhodes, M. R.; Barley, M. H.; Meyer, T. J. *Inorg. Chem.* **1991**, *30*, 629–635. (c) Zang, V.; Eldik, R. *Inorg. Chem.* **1990**, *29*, 4462–4468. (d) Lancon, D.; Kadish, K. M. *J. Am. Chem. Soc.* **1983**, *105*, 5610–5617. (e) Barley, M. H.; Takeuchi, K. J.; Meyer, T. J. *J. Am. Chem. Soc.* **1986**, *108*, 5876–5885. (f) Barley, M. H.; Rhodes, M. R.; Meyer, T. J. *Inorg. Chem.* **1987**, *26*, 1746–1750. (g) Choi, I.-K.; Liu, Y.; Feng, D.; Paeng, K.-J.; Ryan, M. D. *Inorg. Chem.* **1991**, *30*, 1832–1839. (h) Finnegan, M. G.; Lappin, A. G.; Scheidt, W. R. *Inorg. Chem.* **1990**, *29*, 181–185. (i) Nasri, H.; Goodwin, J. A.; Scheidt, W. R. *Inorg. Chem.* **1990**, *29*, 185–191. (j) Nasri, H.; Wang, Y.; Huynh, B. H.; Scheidt, W. R. *J. Am. Chem. Soc.* **1991**, *113*, 717–719. (k) Nasri, H.; Wang, Y.; Huynh, B. H.; Walker, F. A.; Scheidt, W. R. *Inorg. Chem.* **1991**, *30*, 1483–1489.

(6) Aspects of copper NiR activity have been modeled, but with dicopper compounds: (a) Paul, P. P.; Tyeklar, Z.; Farooq, A.; Karlin, K. D.; Liu, S.; Zubieta, J. *J. Am. Chem. Soc.* **1990**, *112*, 2430–2432. (b) Paul, P. P.; Karlin, K. D. *J. Am. Chem. Soc.* **1991**, *113*, 6331–6332.

terization of a model for the *A. cycloclastes* NiR enzyme–substrate complex, a copper–nitrite species stabilized by $[HB(t\text{-}Bupz)_3]^-$, which contains a facially coordinating group of pyrazoles that closely mimic the pyramidal array of histidyl imidazoles coordinated to the active site copper ion in the enzyme.[9] In preliminary explorations of the reactivity of this complex, substitution of nitrite by a labile triflate ligand has been effected, yielding a novel tetrahedral Cu(II) compound with unusual redox properties and great potential as a starting material for further NiR modeling studies.

Addition of a solution of $K[HB(t\text{-}Bupz)_3]$[10] in MeOH to an aqueous solution of equimolar quantities of $CuCl_2$ and $NaNO_2$ resulted in the immediate formation of $[HB(t\text{-}Bupz)_3]Cu(NO_2)$ (**1**) (Scheme I).[11] Despite the demonstrated propensity of the *tert*-butyl-substituted ligand to favor tetrahedral geometries in its transition-metal complexes,[10,12,13] an X-ray crystal structure determination (Figure 1) revealed that the Cu(II) ion in **1** is 5-coordinate, with all three pyrazoles of $[HB(t\text{-}Bupz)_3]^-$ and both oxygens of NO_2^- bound to the metal center. The unusual geometry about copper can be described best as distorted trigonal bipyramidal, with O2 and N21 in pseudoaxial positions, O1, N11, and N11′ in the trigonal plane, and significant cis distortion arising from a nitrite bite angle of 58.7 (2)°. Consequences of the latter include displacement of O1 out of the N11–Cu1–N11′ plane (the N21–Cu1–O1 angle is 110.8°) and a O2–Cu1–N21 angle smaller than 180° (169.5°). Notwithstanding these distortions, the mean copper–ligand distance in the trigonal plane (2.146 Å) is significantly longer than the mean axial distance (1.965 Å) as reported previously for Cu(II) complexes with trigonal-bipyramidal stereochemistry.[8i,14] The nitrite ion is relatively symmetrically bound,[8] the O1–Cu1 and O2–Cu1 distances differing by only 0.19 (1) Å and the N–O distances being equivalent to each other within experimental error.

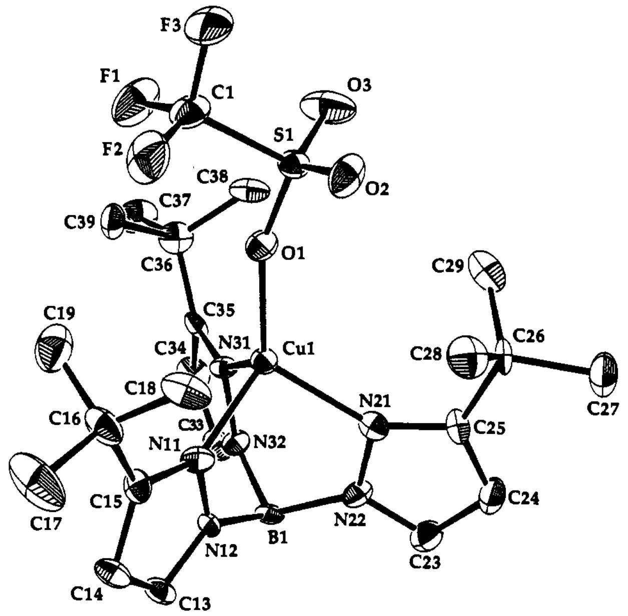

Figure 3. ORTEP drawing of **3** showing the 50% probability thermal ellipsoids and atom labels for all non-hydrogen atoms. Selected interatomic distances (Å) and angles (deg) are as follows: Cu1–O1, 1.947 (7); Cu1–N11, 1.941 (8); Cu1–N21, 2.026 (8); Cu1–N31, 2.042 (8); S1–O1, 1.459 (7); S1–O2, 1.426 (8); S1–O3, 1.423 (9); O1–Cu1–N11, 126.4 (3); O1–Cu1–N21, 121.7 (3); O1–Cu1–N31, 115.4 (3); N11–Cu1–N21, 94.5 (3); N11–Cu1–N31, 93.9 (3); N21–Cu1–N31, 98.5 (3); S1–O1–Cu1, 159.2 (5). Dihedral angles (deg): O1–Cu1–N11/N21–Cu1–N31, 89.8; O1–Cu1–N21/N11–Cu1–N31, 86.4; O1–Cu1–N31/N11–Cu1–N21, 86.7.

An unusual geometry for **1** in solution is indicated by its X-band EPR spectrum (Figure 2a), which contains a rhombic signal with currently ill-understood features that sharply contrasts with the axial spectrum seen for other 5-coordinate, typically square-pyramidal Cu(II) complexes supported by, for example, $[HB(3,5\text{-}diisopropylpz)_3]^-$.[9c,d] The EPR spectrum of $[HB(t\text{-}Bupz)_3]Cu(OAc)$, **2**,[15] a compound topologically analogous to **1**, is particularly noteworthy (Figure 2b), the observed features clearly indicating a square-pyramidal geometry and thus bidentate coordination of acetate.[16] Differences in EPR spectroscopic properties and coordination geometry between **1** and **2** appear to be due to subtle effects that are electronic in origin, since chelating nitrite and acetate exhibit similar bite angles[17] yet because of differences in the electronegativity of their respective central atoms (C vs. N) would be expected to have dissimilar electron donating properties.

The coordination mode of nitrite in **1**, which represents a possible substrate-binding arrangement in copper NiR, diverges significantly from the N-bonded arrangement found in iron–porphyrin adducts suggested as models for heme iron NiRs.[5i–k] We therefore speculate that there may be other significant differences among the copper and iron enzyme catalyzed reaction pathways and intermediates. On the other hand, substantial

---

(7) Carrier, S, M.; Ruggiero, C. R.; Tolman, W. B. Submitted for publication.

(8) Copper(II)–nitrite complexes with nonbiomimetic coligands: (a) Isaacs, N. W.; Kennard, C. H. L. *J. Chem. Soc. A* **1969**, 386–389. (b) Klanderman, K. A.; Hamilton, W. C.; Bernal, I. *Inorg. Chim. Acta* **1977**, *23*, 117–129. (c) Cullen, D. L.; Lingafelter, E. C. *Inorg. Chem.* **1971**, *10*, 1264–1268. (d) Takagi, S.; Joesten, M. D.; Lenhert, P. G. *Acta Crystallogr.* **1975**, *B31*, 596–598. (e) Takagi, S.; Joesten, M. D.; Lenhert, P. G. *J. Am. Chem. Soc.* **1975**, *97*, 444–445. (f) Klein, S.; Reinen, D. *J. Solid State Chem.* **1980**, *32*, 311–319. (g) Mullen, D.; Heger, G.; Reinen, D. *Solid State Commun.* **1975**, *17*, 1249–1252. (h) Procter, I. M.; Stephens, F. S. *J. Chem. Soc. A* **1969**, 1248–1255. (i) Walsh, A.; Walsh, B.; Murphy, B.; Hathaway, B. J. *Acta Crystallogr.* **1981**, *B37*, 1512–1520. (j) Stephens, F. S. *J. Chem. Soc. A* **1969**, 2081–2087.

(9) Analogous ligands have been used to model other copper protein active sites: (a) Kitajima, N.; Fujisawa, K.; Moro-oka, Y. *J. Am. Chem. Soc.* **1989**, *111*, 8975–8976. (b) Kitajima, N.; Koda, T.; Iwata, Y.; Moro-oka, Y. *J. Am. Chem. Soc.* **1990**, *112*, 8833–8839. (c) Kitajima, N.; Fujisawa, K.; Moro-oka, Y. *J. Am. Chem. Soc.* **1990**, *112*, 3210–3212. (d) Kitajima, N.; Fujisawa, K.; Moro-oka, Y. *Inorg. Chem.* **1990**, *29*, 357–358. (e) Thompson, J. S.; Marks, T. J.; Ibers, J. A. *J. Am. Chem. Soc.* **1979**, *101*, 4180.

(10) Trofimenko, S.; Calabrese, J. C.; Thompson, J. S. *Inorg. Chem.* **1987**, *26*, 1507–1514.

(11) $[HB(t\text{-}Bupz)_3]Cu(NO_2)$ (**1**). Anal. Calcd for $C_{21}H_{34}BCuN_7O_2$: C, 51.38; H, 6.98; N, 19.97. Found: C, 51.50; H, 7.16; N, 19.95. UV–vis (CH_2Cl_2) [λ_{max}, nm (ϵ, cm^{-1} M^{-1}): 230 (11 000), 304 (1650), 396 (400), 830 (100). FTIR (KBr, cm^{-1}): 731, 772, 1054, 1167 [$\nu_s(NO_2)$; $\nu_s(^{15}NO_2) = 1164$], 1198, 1259, 1307 [$\nu_{as}(NO_2)$; $\nu_{as}(^{15}NO_2) = 1285$], 1365, 1503, 2484 ($\nu_{BH}$), 2961. Crystal data for **1** ($C_{21}H_{34}BCuN_7O_2$): size 0.60 × 0.40 × 0.25 mm, $M_r = 490.90$, space group *Pnma* (No. 62), at 24 °C, $a = 15.987$ (7) Å, $b = 17.178$ (4) Å, $c = 9.233$ (5) Å, $V = 2536$ (3) Å^3, $Z = 4$, $\rho_{calcd} = 1.286$ g cm^{-3}. For a total of 1530 unique, observed reflections with $I > 3\sigma(I)$ and 164 variable parameters, the current discrepancy indices are $R = 0.052$ and $R_w = 0.062$. Full tables of bond lengths and angles, as well as atomic positional and thermal parameters, for **1** are provided in the supplementary material.

(12) Han, R.; Parkin, G. *Organometallics* **1991**, *10*, 1010–1020 and references therein.

(13) Additional metal–ligand interactions that effectively increase coordination numbers to greater than four in complexes of $[HB(t\text{-}Bupz)_3]^-$ and a related ligand[13b] have been reported: (a) Alsfasser, R.; Powell, A. K.; Vahrenkamp, H. *Angew. Chem., Int. Ed. Engl.* **1990**, *29*, 898–899. (b) Egan, J. W., Jr.; Haggerty, B. S.; Rheingold, A. L.; Sendlinger, S. C.; Theopold, K. H. *J. Am. Chem. Soc.* **1990**, *112*, 2445–2446.

(14) Huq, F.; Skapski, A. C. *J. Chem. Soc. A* **1971**, 1927.

(15) $[HB(t\text{-}Bupz)_3]Cu(OAc)$ (**2**) (prepared via treatment of $Tl[HB(t\text{-}Bupz)_3]$ with $Cu(OAc)_2{\cdot}H_2O$ in THF/MeOH). Anal. Calcd for $C_{23}H_{37}BCuN_6O_2$: C, 54.82; H, 7.40; N, 16.68. Found: C, 55.21; H, 7.36; N, 17.14. UV–vis (CH_2Cl_2) [λ_{max}, nm (ϵ, cm^{-1} M^{-1}): 236 (4400), 292 (3080), 784 (110). FTIR (KBr, cm^{-1}): 622, 697, 732, 1063, 1170, 1201, 1258, 1364, 1460, 1482 (ν_{COO}), 1505, 1527 (ν_{COO}), 2488 (ν_{BH}), 2965.

(16) Similar properties are exhibited by a related copper(II) carboxylate complex that was structurally characterized.[9d] Bidentate acetate coordination in the Cu(II) complexes contrasts with the apparent η^1 mode observed for (a) $[HB(t\text{-}Bupz)_3]Zn(OAc)$: Gorrell, I.; Looney, A.; Parkin, G. *J. Chem. Soc., Chem. Commun.* **1990**, 220–222, and (b) $[HB(t\text{-}Bupz)_3]Mg(OAc)$: Han, R.; Looney, A.; Parkin, G. *J. Am. Chem. Soc.* **1989**, *111*, 7276–7278.

(17) Poganiuch, P.; Liu, S.; Papaefthymiou, G. C.; Lippard, S. J. *J. Am. Chem. Soc.* **1991**, *113*, 4645–4651 and references therein.

molecular rearrangements are clearly necessary for conversion of an *O,O*-nitrite to a *N*-nitrosyl (a transformation we have yet to observe for model complex **1**), suggesting that *N*-nitrite coordination may be more productive in denitrification mechanisms. Experiments designed to test this idea are in progress.

Preliminary investigation of the reactivity of **1** indicates that the coordinated nitrite is readily displaced. For example, addition of (PPN)Cl to a solution of **1** in CH_3CN resulted in quantitative formation of $[HB(t\text{-Bupz})_3]CuCl$ (UV-vis).[10] In a reaction originally attempted in order to model the proton-induced dehydration suggested as the initial step in enzymatic nitrite reduction,[4] treatment of **1** with TMSOTf instead induced nitrite removal (presumably as the TMS ester) and formation of deep purple $[HB(t\text{-Bupz})_3]CuOTf$ (**3**) (62%, Scheme I).[18] Compound **3** was also prepared independently by the reaction of $[HB(t\text{-Bupz})_3]CuCl$ with AgOTf. An X-ray structure determination of **3**·C_7H_8 revealed monodentate triflate bonding[19] to a Cu(II) ion that adopts a rare tetrahedral coordination geometry (Figure 3).[7,9c,20] The coordination sphere of the complex is similar to that of $[HB(3,5\text{-diisopropylpz})_3]CuCl$ (**4**),[9c] the only significant deviations from an ideal tetrahedral arrangement for **3** being intraligand angles between the pyrazole nitrogen donor atoms that are less than, and O1–Cu–N angles that are more than, 109.5° (average N–Cu–N = 97.2° and average O1–Cu–N = 121.2°). Like **4**, dihedral angles for **3** closely approach 90° (avg. 87.6°), in contrast to the lesser angles reported for other more distorted tetrahedral Cu(II) complexes.[20] EPR spectroscopic data for **3** (Figure 2c) and **4**[9c] in noncoordinating solvents are also similar, both compounds exhibiting signals that support retention of tetrahedral geometries in solution.[21]

Cyclic voltammetry of **3** in 0.1 M Bu_4NOTf in CH_2Cl_2/CH_3CN ($\sim$9:1) revealed an electrochemically quasi-reversible ($\Delta E_{pp} = 110$ mV, greater values at scan rates >50 mV/s) and chemically reversible ($i_{pc}/i_{pa} \approx 1$) reduction with $E_{1/2} = +0.91$ V vs SCE. An identical cyclic voltammogram was obtained by starting with $[HB(t\text{-Bupz})_3]Cu(CH_3CN)$ (**5**),[7] clearly identifying it as the reduction product. Only an irreversible reduction at +0.55 V was observed for **3** in the absence of added CH_3CN, suggesting that **5** is reversibly formed by reduction of a CH_3CN adduct of **3**. In support of this hypothesis, significant changes in the spectroscopic features of **3** (UV–vis, EPR) occur upon dissolution in CH_3CN, although we have not yet isolated and definitively characterized the apparent triflate substitution product. The redox potential for the **3**·$CH_3CN \leftrightarrow$ **5** process is extraordinarily large and positive, presumably because geometric constraints (e.g. tetrahedral distortion) destabilize the Cu(II) state.[22] Future work will address this possibility as well as further aspects of the biomimetic reactivity of **1** and potential use of **5** as an oxidant and starting material for the synthesis of additional monocopper NiR model complexes.

Acknowledgment. I thank Professor Doyle Britton for his work on the X-ray structures of **1** and **3**, Christy Ruggiero for her help with EPR data collection, Professors Elinor T. Adman, Kenneth D. Karlin, and Bruce A. Averill for sending preprints (refs 3, 6b, and 4c, respectively), and the University of Minnesota for financial support.

Supplementary Material Available: Tables of atomic positional and isotropic thermal parameters, anisotropic thermal parameters, bond lengths, and bond angles for **1** and **3**·C_7H_8 (20 pages). Ordering information is given on any current masthead page.

Department of Chemistry
University of Minnesota
Minneapolis, Minnesota 55455

William B. Tolman

Received July 26, 1991

---

(18) $[HB(t\text{-Bupz})_3]Cu(OTf)\cdot C_7H_8$ (**3**·C_7H_8). Anal. Calcd for $C_{29}H_{42}BCuF_3N_6O_3S$: C, 50.77; H, 6.17; N, 12.25. Found: C, 49.05; H, 5.96; N, 12.40 (replicate analyses also gave low values for carbon, suggesting unavoidable partial loss of toluene solvate). UV–vis (CH_2Cl_2) [λ_{max}, nm (ϵ, $cm^{-1}\,M^{-1}$): 234 (7800), 256 (2600), 292 (sh, 1550), 434 (350), 550 (350). FTIR (KBr, cm^{-1}): 632, 731, 781, 1012 (ν_{SO}), 1058, 1198, 1236 (ν_{SO}), 1258, 1341 (ν_{SO}), 1367, 1501, 2511 (ν_{BH}), 2966. Crystal data for **3**·C_7H_8 ($C_{29}H_{42}BCuF_3N_6O_3S$): size 0.35 × 0.30 × 0.15 mm, $M_r = 686.10$, space group $P2_1/n$ (No. 14), at −101 °C, $a = 10.367$ (6) Å, $b = 20.555$ (7) Å, $c = 15.39$ (1) Å, $\beta = 90.80$ (5)°, $V = 3279$ (6) Å^3, $Z = 4$, $\rho_{calcd} = 1.390$ cm^{-3}. For a total of 2809 unique, observed reflections with $I > 2\sigma(I)$ and 347 variables, the current discrepancy indices are $R = 0.076$ and $R_w = 0.076$. Full tables of bond lengths and angles, as well as atomic positional and thermal parameters for **3**·C_7H_8 are provided in the supplementary material.

(19) (a) Lawrance, G. A. *Chem. Rev.* **1986**, *86*, 17–33. (b) For other examples of triflate coordination to Cu(II), see: Dedert, P. L.; Thompson, J. S.; Ibers, J. A.; Marks, T. J. *Inorg. Chem.* **1982**, *21*, 969–977, 3506–3517 and references therein.

(20) Knapp, S.; Keenan, T. P.; Zhang, X.; Fikar, R.; Potenza, J. A.; Schugar, H. J. *J. Am. Chem. Soc.* **1990**, *112*, 3452–3464 and references therein.

(21) Parker, I. H. *J. Phys. C: Solid State Phys.* **1971**, *4*, 2967–2978.

(22) (a) Patterson, G. S.; Holm, R. H. *Bioinorg. Chem.* **1975**, *4*, 257–275. (b) Zanello, P. *Comments Inorg. Chem.* **1988**, *8*, 45–78. (c) Bouwman, E.; Driessen, W. L.; Reedijk, J. *Coord. Chem. Rev.* **1990**, *104*, 143–172. (d) Sorrell, T. N.; Jameson, D. L. *Inorg. Chem.* **1982**, *21*, 1014–1019.

A 3-Coordinate 4-Electron Phosphorus Donor[1]

A 3-coordinate phosphorus which can act as a 4-electron donor has never been observed. We have previously reported the synthesis, structure, chemistry[2-12] and electronic structure[13] of ADPnO[14] systems containing 3-coordinate, 10-electron pnictogen centers (10-Pn-3;[15] Pn = P, As, or Sb). The identity of the pnictogen center determines which of two general reactivity categories the molecules follow. The ring systems derived from either arsenic or antimony have been shown to form complexes with transition-metal centers which retain both the planar structure of the ADPnO ring and the hypervalent arrangement at the pnictogen center. Either 10-Pn-4[4,6] or 10-Pn-5[10] complexes can be formed depending on the number of metals which coordinate.

The phosphorus-derived ring system (ADPO) tends to show chemistry in which only a single lone pair of electrons from phosphorus is involved. Chemistry at the phosphorus of ADPO is generally accompanied by a reduction of the tridentate ligand backbone in ADPO by the second lone pair at the phosphorus center. This reduction leads to a folding of the ADPO ring systems in transition-metal complexes.[4,5,7,9-11,13] The unique reactivity of ADPO has been explained in terms of configuration mixing that transfers σ-electron density to the π-systems at phosphorus.[9-11,13]

---

(1) Contribution No. 5950.

(2) Culley, S. A.; Arduengo, A. J., III. *J. Am. Chem. Soc.* **1984**, *106*, 1164. Culley, S. A.; Arduengo, A. J., III. *J. Am. Chem. Soc.* **1985**, *107*, 1089.

(3) Stewart, C. A.; Harlow, R. L.; Arduengo, A. J., III. *J. Am. Chem. Soc.* **1985**, *107*, 5543.

(4) Arduengo, A. J., III; Stewart, C. A.; Davidson, F.; Dixon, D. A.; Becker, J. Y.; Culley, S. A.; Mizen, M. B. *J. Am. Chem. Soc.* **1987**, *109*, 627.

(5) Arduengo, A. J., III; Stewart, C. A.; Davidson, F. *J. Am. Chem. Soc.* **1986**, *108*, 322.

(6) Stewart, C. A.; Arduengo, A. J., III. *Inorg. Chem.* **1986**, *25*, 3847.

(7) Arduengo, A. J., III. *Pure Appl. Chem.* **1987**, *59*, 1053.

(8) Arduengo, A. J., III; Dixon, D. A.; Stewart, C. A. *Phosphorus Sulfur* **1987**, *30*, 341.

(9) Arduengo, A. J., III; Lattman, M.; Calabrese, J. C.; Fagan, P. J. *Heteroat. Chem.* **1990**, *1*, 407.

(10) Arduengo, A. J., III; Lattman, M.; Dias, H. V. R.; Calabrese, J. C.; Kline, M. *J. Am. Chem. Soc.* **1991**, *113*, 1799.

(11) Arduengo, A. J., III; Lattman, M.; Dixon, D. A.; Calabrese, J. C. *Heteroat. Chem.* **1991**, *2*, 395.

(12) Arduengo, A. J., III; Dias, H. V. R.; Calabrese, J. C. *J. Am. Chem. Soc.* **1991**, *113*, 7071.

(13) Arduengo, A. J., III; Dixon, D. A. Electron Rich Bonding at Low Coordination Main Group Element Centers. In *Heteroatom Chemistry: ICHAC-2*; Block, E., Ed.; VCH: New York, 1990; p 47.

(14) The ADPnO acronym has been previously described and is used for simplicity in place of the name of the ring system it represents: 5-*a*za-2,8-*d*ioxa-1-*pn*ictabicyclo[3.3.0]octa-2,4,6-triene. See ref 4, footnote 1d, for details.

(15) The *N*–X–*L* nomenclature system has been previously described (Perkins, C. W.; Martin, J. C.; Arduengo, A. J., III; Lau, W.; Algeria, A.; Kochi, J. K. *J. Am. Chem. Soc.* **1980**, *102*, 7753): *N* valence electrons about a central atom X, with *L* ligands.

0020-1669/91/1330-4880$02.50/0